

Review

Open Access



# Recent advances in electrolyte design for optimized lithium polysulfides solvation in lithium-sulfur batteries

Seung-Yeon Jung<sup>1</sup> , Jun-Young Park<sup>1</sup>, Seung-Ho Yu<sup>1,2,\*</sup>

<sup>1</sup>Department of Chemical and Biological Engineering, Korea University, Seoul 02841, Republic of Korea.

<sup>2</sup>Department of Battery-Smart Factory, Korea University, Seoul 02841, Republic of Korea.

\*Correspondence to: Prof./Dr. Seung-Ho Yu, Department of Chemical and Biological Engineering, Korea University, 145 Anam-ro, Seongbuk-gu, Seoul 02841, Republic of Korea; Department of Battery-Smart Factory, Korea University, 145 Anam-ro, Seongbuk-gu, Seoul 02841, Republic of Korea. E-mail: seunghoyu@korea.ac.kr

**How to cite this article:** Jung, S. Y.; Park, J. Y.; Yu, S. H. Recent advances in electrolyte design for optimized lithium polysulfides solvation in lithium-sulfur batteries. *Energy Mater.* 2025, 5, 500125. <https://dx.doi.org/10.20517/energymater.2025.31>

**Received:** 5 Feb 2025 **First Decision:** 28 Mar 2025 **Revised:** 29 Apr 2025 **Accepted:** 15 May 2025 **Published:** 25 Jun 2025

**Academic Editors:** Yoon Hwa, Yuhui Chen **Copy Editor:** Fangling Lan **Production Editor:** Fangling Lan

## Abstract

Lithium-sulfur (Li-S) batteries have emerged as a promising candidate for next-generation secondary batteries due to their high energy density and cost-effective sulfur cathodes. These batteries operate through electrochemical reactions involving sulfur, during which lithium polysulfides (LiPSs) are formed as liquid-phase intermediates. The solvation behavior of LiPSs plays a crucial role in determining the electrochemical performance and cycling stability of Li-S batteries. Electrolytes, as a key factor, govern the dissolution of LiPSs, with the properties, quantities, and ratios of components playing a critical role in forming the solvation structure of both Li<sup>+</sup> ions and LiPSs. In this review, the extent of LiPS solvation is systematically categorized into highly, sparingly and weakly solvating electrolytes, and the influence of solubility on electrochemical performance is elucidated. Furthermore, the effects of additives and diluents on the solvation structures of LiPSs are analyzed to reveal the underlying mechanisms that govern their electrochemical behavior. This review emphasizes the importance of optimizing LiPS solvation properties through rational electrolyte design to enhance the performance and stability of Li-S batteries, providing valuable insights into the development of advanced electrolyte systems.

**Keywords:** Li-S batteries, solvation property, polysulfide solubility, electrolyte



© The Author(s) 2025. **Open Access** This article is licensed under a Creative Commons Attribution 4.0 International License (<https://creativecommons.org/licenses/by/4.0/>), which permits unrestricted use, sharing, adaptation, distribution and reproduction in any medium or format, for any purpose, even commercially, as long as you give appropriate credit to the original author(s) and the source, provide a link to the Creative Commons license, and indicate if changes were made.



## INTRODUCTION

Lithium-ion batteries (LIBs) have long dominated the commercial energy storage market, particularly in consumer electronics and electric vehicles<sup>[1-3]</sup>. However, the theoretical energy density of LIBs (387 Wh kg<sup>-1</sup>) poses an inherent limitation, underscoring the necessity for next-generation battery technologies<sup>[4,5]</sup>. Among the emerging alternatives, Lithium-sulfur (Li-S) batteries have garnered significant attention owing to their high theoretical energy density (2,567 Wh kg<sup>-1</sup>), as well as the low cost, abundance, and eco-friendly nature of sulfur as a cathode material. In contrast to LIBs, which operate based on intercalation reactions, Li-S batteries rely on the conversion reactions of sulfur. In ether-based electrolytes, the discharge process begins with the sequential reduction of solid sulfur (S<sub>8</sub>) to form soluble polysulfides (Li<sub>2</sub>S<sub>x</sub>, 3 ≤ x ≤ 8), followed by the formation of Li<sub>2</sub>S<sub>2</sub> and Li<sub>2</sub>S<sup>[6-8]</sup>. The intermediate products in these reactions are soluble polysulfides in the electrolyte, which exist in various forms such as dianions (S<sub>n</sub><sup>2-</sup>), monoanions (S<sub>n</sub><sup>-</sup>), radicals (S<sub>n</sub><sup>•</sup>) and their clusters. The presence and dominance of radical species depend on the solvent polarity. Due to their high nucleophilicity, lithium polysulfides (LiPSs) preferentially interact with electrophilic solvents. One of the key parameters determining a solvent's electrophilicity is its donor number (DN). Solvents with high DN stabilize a wide range of polysulfide species and particularly facilitate redox reactions by stabilizing radicals<sup>[9,10]</sup>. As such, LiPSs play a pivotal role in determining redox kinetics, and the types of stable species present can significantly influence the discharge capacity.

While LiPSs are essential for the operation of Li-S batteries, they also introduce several challenges. Upon dissolving in ether-based electrolytes, LiPSs can shuttle between electrodes, resulting in active material loss and reduced cycle life. Additionally, polysulfides migrating to the anode may undergo parasitic reactions with Li, leading to corrosion and an increase in inactive Li. The precipitation of insoluble Li<sub>2</sub>S on the electrode surface further blocks electron transport, reducing active surface area and lowering Coulombic efficiency, which can ultimately lead to cell failure<sup>[11,12]</sup>.

Given the critical role of LiPSs throughout the discharge-charge process, controlling their behavior is essential. The solubility of LiPSs influences polarization, sulfur utilization, and solid-electrolyte interphase (SEI) formation, all of which directly affect battery performance<sup>[13,14]</sup>. Since the electrolyte is the primary factor determining LiPS solubility, controlling its composition and physicochemical properties is crucial. A well-designed electrolyte can suppress excessive LiPS dissolution and mitigate the shuttle effect without compromising sulfur redox kinetics<sup>[15]</sup>.

A key factor in electrolyte design is the solvation structure. When a lithium salt dissolves in a solvent, it dissociates into Li<sup>+</sup> and the corresponding anion, simultaneously forming a solvation shell around the Li<sup>+</sup> [Figure 1A]. Three major types of Li<sup>+</sup> solvation structures - solvent-separated ion pair (SSIP), contact ion pair (CIP), or aggregate (AGG) - can coexist, with their relative proportions depending on the electrolyte composition. Recent studies have focused on promoting CIP and AGG structures to facilitate the formation of anion-derived SEI layers<sup>[16,17]</sup>. In Li-S batteries, it is also essential to consider the solvation structure of soluble LiPSs [Figure 1B]. When LiPSs dissolve, solvent molecules or anions coordinate with the Li<sup>+</sup> at the terminal ends of the polysulfide chain<sup>[18,19]</sup>. Under low-temperature or lean-electrolyte conditions, LiPS clusters are likely to form. Understanding and tuning these solvation interactions are critical for optimizing battery performance.

Given this complexity of Li-S batteries, various electrolyte design strategies have been developed, categorized based on their ability to dissolve LiPSs - specifically, highly solvating electrolytes (HSEs), sparingly solvating electrolytes (SSEs), and weakly solvating electrolytes (WSEs)<sup>[20-22]</sup>. A summarized schematic illustrating the internal cell processes affected by the solubility of LiPSs is shown in Figure 1C. In

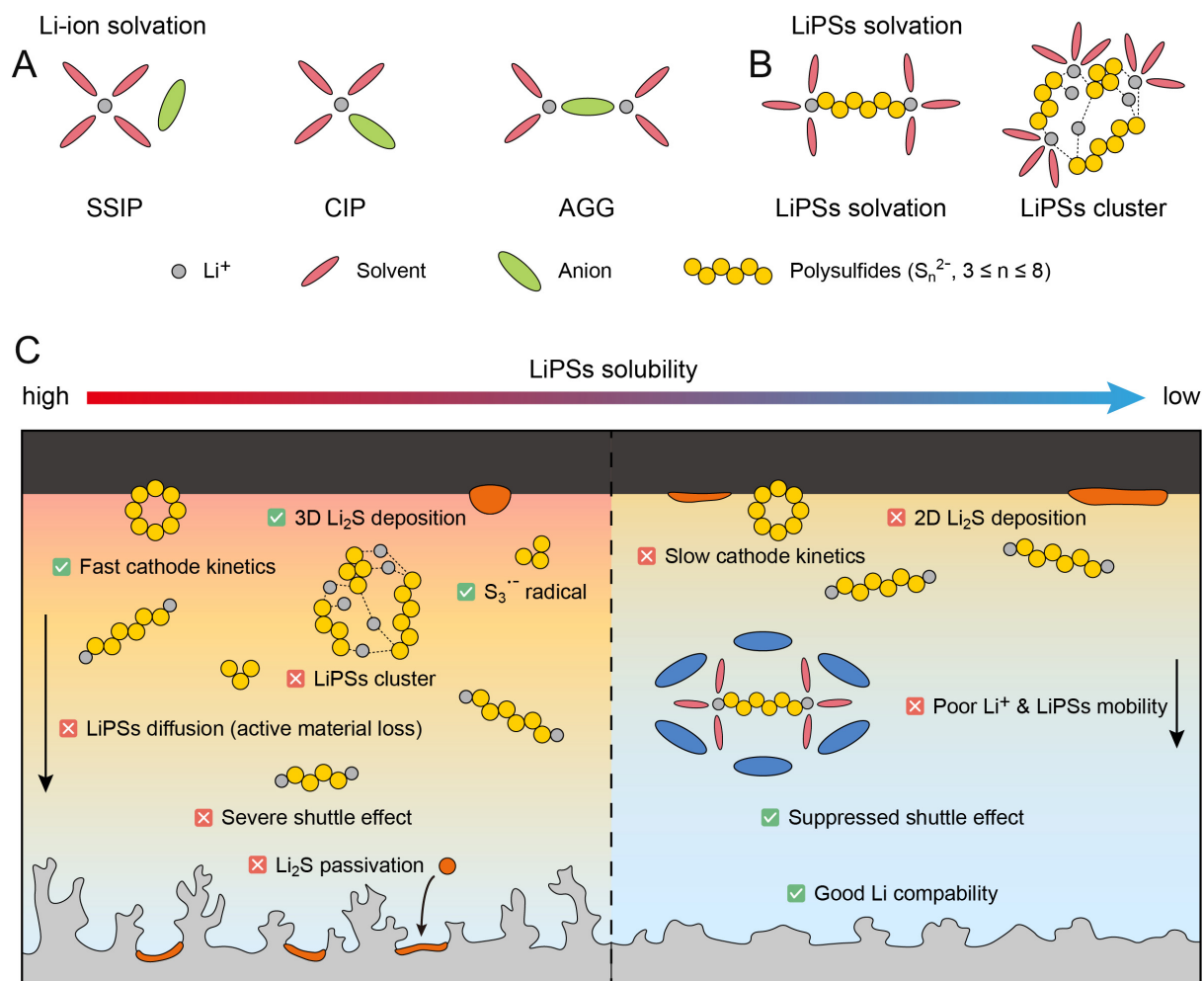


**Figure 1.** (A) Schematic representations for Li-ion solvation structures; solvent-separated ion pair (SSIP), contact ion pair (CIP), aggregate (AGG). (B) Schematic representations for LiPSs solvation and LiPSs cluster. (C) Schematic showing the characteristics of electrolytes with high and low LiPSs solubility.

HSEs, LiPSs dissolve extensively into the electrolyte, leading to significant diffusion from the cathode to the anode. This excessive dissolution exacerbates the shuttle effect, requiring strategies such as electrolyte optimization and the incorporation of functional additives. Furthermore, solvents specifically designed to mitigate lithium metal corrosion are employed to address the adverse effects of LiPSs diffusion in HSEs<sup>[23-25]</sup>. In contrast, SSEs effectively suppress LiPSs dissolution, mitigating the shuttle effect. However, the limited solubility of LiPSs in SSEs also slows cathode reactions, necessitating strategies to enhance reaction kinetics, such as the use of diluents or optimized electrochemical processes<sup>[26,27]</sup>. To balance the advantages and drawbacks of HSEs and SSEs, WSEs have been proposed. These electrolytes allow moderate LiPSs solubility, aiming to minimize the polysulfide shuttle effect while maintaining sufficient solubility to support fast reaction kinetics<sup>[28,29]</sup>.

This review explores how the distinct solvation structures of Li<sup>+</sup> and the solvation behavior of LiPSs influence the performance of Li-S batteries in HSEs, SSEs, and WSEs. We also examine strategies for enhancing Li-S battery performance through electrolyte design. Given the critical role of LiPSs dissolution in determining key performance parameters - such as polarization, sulfur utilization, shuttle effect

suppression, and electrode stability - we emphasize the importance of tailoring electrolyte compositions to achieve an optimal balance. By addressing these challenges through innovative electrolyte strategies, the performance and stability of Li-S batteries can be significantly improved.

## SOLVATION CHEMISTRY AND ELECTROCHEMICAL BEHAVIOR

The conversion reaction in Li-S batteries is driven by differences in Gibbs free energy ( $\Delta G$ ) and is distinctly reflected in the voltage profile as two separate plateaus. During the discharge process, the 1st plateau represents the reduction of  $S_8$  to soluble liquid-phase LiPSs, while the 2nd plateau corresponds to the subsequent reduction of these soluble LiPSs into insoluble  $Li_2S_2$  or  $Li_2S$ . The solubility and thermodynamic stability of LiPSs directly influence the electrochemical characteristics of these plateaus. The Nernst equation ( $\Delta G = -nFE$ ) demonstrates how changes in Gibbs free energy influence the voltage profile, highlighting its significance in electrochemical reactions. As the discharge process progresses from  $S_8$  to  $Li_2S$ , the Gibbs free energy difference in the dissolution reaction from  $S_8$  to soluble LiPSs corresponds to the voltage of the 1st plateau, while the Gibbs free energy difference in the precipitation reaction from soluble LiPSs to  $Li_2S$  corresponds to the voltage of the 2nd plateau, as defined by the Nernst equation. In other words, a larger Gibbs free energy difference corresponds to a higher voltage for the respective plateau, while a smaller difference results in a lower voltage<sup>[30]</sup>.

In HSEs, the ratio of solvent molecules is significantly higher compared to lithium salts or additive molecules, leading to an abundance of free solvent molecules. These solvent molecules typically possess a high DN or high dielectric constant ( $\epsilon$ ), which enable strong electron-donating properties. This results in strong interactions with  $Li^+$  ions, promoting their solvation and leading to the predominant formation of SSIP [Figure 2A].  $S_3^{\cdot-}$  radicals, predominantly generated in HSEs, provide an additional reaction pathway beyond the conventional sulfur redox pathway through LiPSs, thereby enhancing redox activity. In HSEs, both  $Li^+$  ions and LiPSs are thermodynamically stabilized when dissolved, making the dissolution reaction more spontaneous. The thermodynamic stability of LiPSs indicates lower Gibbs free energy, resulting in an increased Gibbs free energy difference with  $S_8$ , while the difference with  $Li_2S$  decreases. This leads to a relatively higher voltage for the 1st plateau and a relatively lower voltage for the 2nd plateau [Figure 2B]<sup>[31,32]</sup>.

In contrast, SSEs are designed to suppress LiPSs solubility, resulting in an excess of anions generated by lithium salts or additives and a significant reduction in free solvent molecules. Furthermore, since the solvent molecules used in SSEs typically have a low DN or low dielectric constant, their electron-donating ability is weak, leading to poor coordination with  $Li^+$  ions. Consequently, solvation structures such as CIP and AGG, where both solvents and anions coordinate with  $Li^+$  ions, become predominant. Due to the insufficient number of solvents and the weak electron-donating capability of the solvents in SSEs, the thermodynamic stability of LiPSs is relatively low, resulting in higher Gibbs free energy for LiPSs. This leads to a smaller Gibbs free energy difference with  $S_8$  and a larger difference with  $Li_2S$ , causing the 1st plateau to appear at a relatively lower voltage and the 2nd plateau at a relatively higher voltage.

Understanding these electrochemical phenomena requires a comprehensive investigation of solvation structures within the electrolyte. The distribution of these structures is influenced by electrolyte properties such as solvent composition, ionic concentration, and operational conditions. For instance, environments with high solvent availability and low anion concentrations favor the formation of SSIP, enhancing the solubility of LiPSs. In contrast, conditions with limited solubility and high anion concentrations promote the prevalence of CIP and AGG structures. The dissolution of LiPSs introduces additional complexity. When the LiPS clusters form, their size and thermodynamic stability significantly affect polysulfide diffusion and reaction kinetics, ultimately influencing electrochemical performance. Electrolyte

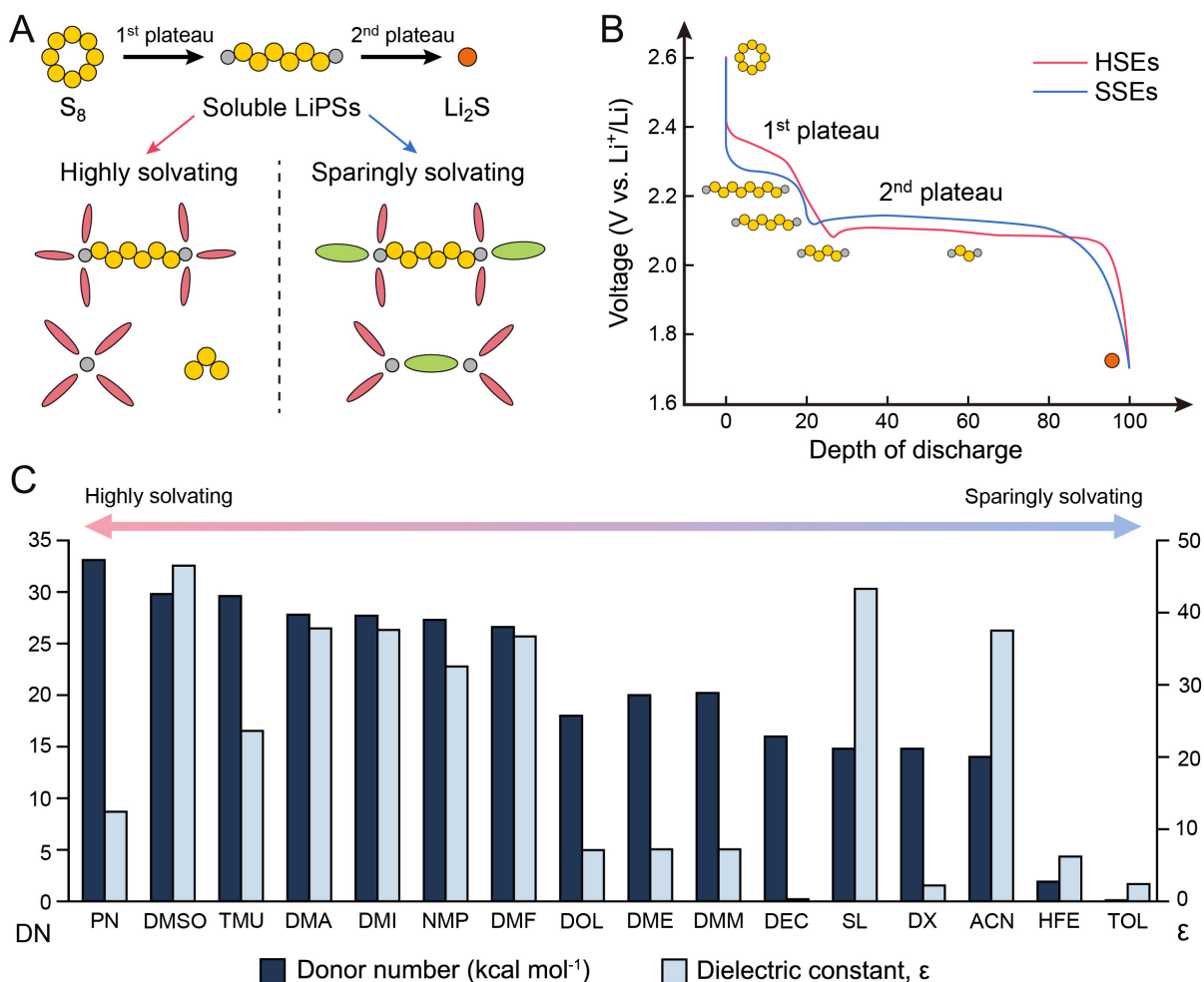


**Figure 2.** Properties of highly and sparingly (including weakly) solvating solvents. (A) Schematic of highly and sparingly solvating soluble LiPSs. (B) Voltage profile of HSEs and SSEs. This figure is modified with Kim et al.<sup>[31]</sup> Copyright 2024, Springer Nature. (C) Donor number and dielectric constant of solvents. PN: Pyridine; DMSO: dimethyl sulfoxide; TMU: tetramethylurea; DMA: dimethylacetamide; DMI: 1,3-dimethyl-2-imidazolidinone; NMP: N-methyl-2-pyrrolidone; DMF: N,N-dimethylformamide; DOL: 1,3-dioxolane; DME: 1,2-dimethoxyethane; DMM: dimethoxymethane; DEC: diethyl carbonate; SL: sulfolane; DX: 1,4-dioxane; ACN: acetonitrile; HFE: hydrofluoroether; TOL: toluene.

concentration is a key factor in solvation dynamics. In highly dilute systems, the prevalence of SSIPs facilitates LiPSs dissolution, whereas in concentrated electrolytes, CIP and AGG structures dominate, restricting LiPSs solubility. Lean-electrolyte configurations, characterized by a low electrolyte-to-sulfur (E/S) ratio, exacerbate these effects by limiting solvent availability, reducing polysulfide dissolution and altering reaction pathways<sup>[21,33,34]</sup>. Recent studies have extensively focused on optimizing these conditions to balance polysulfide solubility and mitigate shuttle effects.

The dielectric constant has traditionally been a useful metric for assessing electrolyte performance, particularly in terms of lithium salt solubility and ion dissociation<sup>[35,36]</sup>. While solvents with high dielectric constant, such as ethylene carbonate (EC) and sulfolane (SL), generally exhibit good ionic conductivity, their ability to dissolve LiPSs does not always correlate with their dielectric properties<sup>[37]</sup>. For example, solvents like pyridine (PN) and tetramethylurea (TMU), despite having relatively low dielectric constant, outperform high- $\epsilon$  solvents in terms of polysulfide solubility. This highlights that dielectric constant alone

may not fully explain the complex factors governing electrolyte behavior, particularly concerning LiPSs solubility in Li-S batteries.

DN, introduced by Gutmann, complements the dielectric constant by providing a more reliable parameter for evaluating solvation characteristics<sup>[38]</sup>. DN quantifies the electron-donating ability of a solvent or anion, effectively capturing its interaction strength with electron acceptors such as  $\text{Li}^+$  ions. Solvents with high DN values, such as dimethylacetamide (DMA) or dimethyl sulfoxide (DMSO), exhibit strong coordination with  $\text{Li}^+$  ions, promoting favorable solvation structures and enhancing LiPSs solubility<sup>[39]</sup>. 1,3-Dioxolane (DOL) and 1,2-dimethoxyethane (DME), commonly used as electrolytes in Li-S batteries, have medium DN values and dielectric constants below 10, in comparison to other solvents. In contrast, low-DN solvents tend to suppress polysulfide dissolution, which can be advantageous for reducing the shuttle effect. [Figure 2C](#) illustrates how considering DN alongside the dielectric constant provides a more comprehensive understanding of LiPSs solubility, emphasizing DN's utility as a key guiding principle in electrolyte design.

Finally, the interplay between LiPSs formation, solvation structure, Gibbs free energy differences, and voltage profiles is intrinsically interconnected, collectively determining the electrochemical performance and stability of Li-S batteries. Systematic optimization of electrolyte composition and operational parameters allows researchers to balance shuttle suppression with reaction kinetics, thereby enhancing battery performance. This comprehensive understanding of solvation fundamentals forms the foundation for developing innovative electrolyte designs that address the unique challenges of Li-S technology.

## ELECTROLYTE DESIGN STRATEGIES BASED ON POLYSULFIDE SOLUBILITY

In this section, we discuss electrolyte design strategies with a focus on LiPSs solubility and their impact on electrochemical performance. The degree of LiPSs solvation plays a crucial role in determining cycling stability, sulfur redox kinetics, and shuttle effect in Li-S batteries. Based on the solvation ability, electrolytes can be classified as highly, sparingly, and WSEs. Each category presents distinct advantages and limitations, influencing battery performance in different ways. The following sections provide a detailed discussion on these electrolyte types, highlighting their characteristics and potential strategies for optimizing their effects.

### Highly solvating electrolytes

HSEs are particularly effective for enhancing cathode kinetics in Li-S batteries. As illustrated in [Figure 3A](#), the significant presence of dissolved LiPSs shifts the solid-solid conversion pathway to the solid-liquid-solid conversion pathway, leading to improved sulfur utilization and faster conversion kinetics. A distinct feature of HSEs is their ability to facilitate the formation of  $\text{S}_3^{\cdot-}$  radicals, which exhibit significantly higher reactivity compared to dissolved polysulfide anions<sup>[25,40]</sup>. Moreover, HSEs promote three-dimensional (3D)  $\text{Li}_2\text{S}$  deposition, which mitigates  $\text{Li}_2\text{S}$  passivation and enables rapid precipitation and dissolution reactions, thus enhancing  $\text{Li}_2\text{S}$  utilization. However, the high solubility of LiPSs in HSEs can lead to the diffusion of soluble LiPS species, resulting in active material loss. This phenomenon contributes to undesired side reactions with lithium metal, causing lithium metal corrosion,  $\text{Li}_2\text{S}$  passivation, and the formation of severe Li dendrites. To overcome these limitations, various strategies have been extensively investigated. Shen *et al.* developed HSEs using a fluorenone (FL) additive, which captures and stabilizes  $\text{S}_3^{\cdot-}$  radicals<sup>[41]</sup>. This stabilization increases the concentration of soluble LiPSs and enhances their reactivity. [Figure 3B](#) and [C](#) illustrates that *in-situ* Raman spectroscopy reveals the accelerated disappearance of  $\text{S}_8$  and enhanced capture of  $\text{S}_3^{\cdot-}$  radicals upon the addition of FL. The increased concentration of  $\text{S}_3^{\cdot-}$  radicals results in a more rapid reduction of polysulfide anions, demonstrating that the presence of  $\text{S}_3^{\cdot-}$  radicals significantly enhances redox activity, thereby improving sulfur utilization. The marked reduction of polysulfide anion peaks in the spectra confirms the successful conversion of LiPSs to  $\text{Li}_2\text{S}$ . These findings highlight that HSEs, particularly through

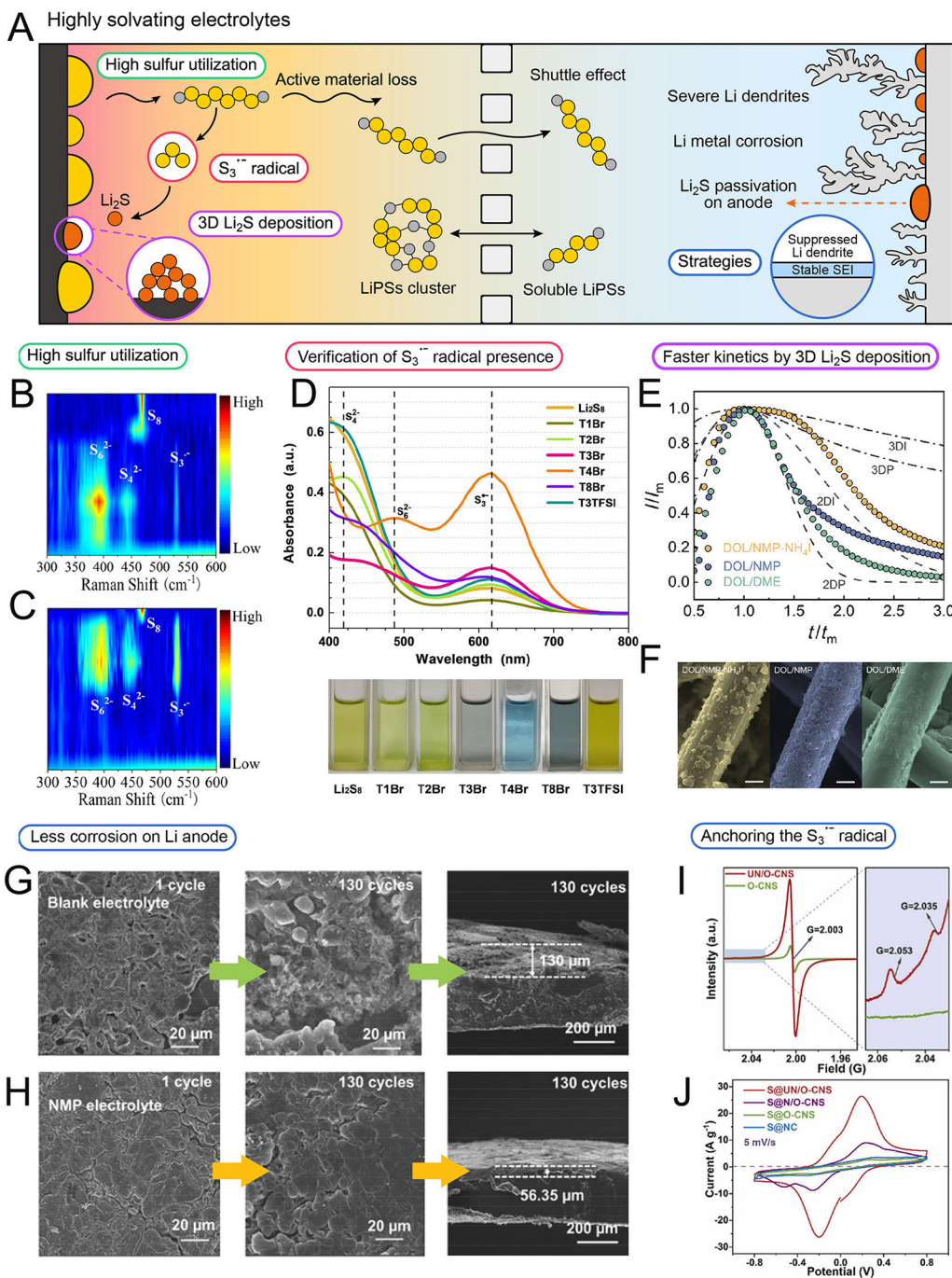


**Figure 3.** (A) Schematic of advantages and challenges of using HSEs in Li-S batteries. *In-situ* Raman spectra of the Li-S batteries at a 1 C rate: (B) without FL and (C) with FL. These figures are quoted and reproduced from Shen et al.<sup>[41]</sup> Copyright 2023, Elsevier B.V.; (D) UV-vis spectra and photographs of the  $Li_2S_8$  solution after contact with quaternary ammonium salts T1Br, T2Br, T3Br, T4Br, T8Br, and T3TFSI. This figure is quoted and reproduced from Meng et al.<sup>[42]</sup> Copyright 2023, Wiley-VCH GmbH; (E) Corresponding dimensionless current-time profiles as well as the curves for theoretical 2D and 3D nucleation model. (F) SEM images of precipitated  $Li_2S$  on the CP substrate after PITT discharge process (Scale bar:  $\mu m$ ). These figures are quoted and reproduced from Shi et al.<sup>[43]</sup> Copyright 2024, Tsinghua University Press; SEM images of the surface and cross-section morphology of lithium metal after 1, 130 cycles in (G) DOL/DME electrolyte and (H) 1 vol% of NMP in DOL/DME electrolyte. These figures are quoted and reproduced from Zhong et al.<sup>[44]</sup> Copyright 2022, Wiley-VCH GmbH; (I) EPR spectra of UN/O-CNS and O-CNS. (J) CV curves of symmetric cells with  $Li_2S_6$  electrolyte under a scan rate of  $5 mV s^{-1}$ . These figures are quoted and reproduced from Cui et al.<sup>[45]</sup> Copyright 2024, Elsevier Ltd.

the generation of  $S_3^{\cdot-}$  radicals, significantly improve sulfur utilization. The formation of  $S_3^{\cdot-}$  radicals in HSEs can be identified using UV-vis spectroscopy and visual observation. Polysulfide dianions and  $S_3^{\cdot-}$  radicals exhibit characteristic peaks in the UV-vis spectra:  $S_8^{2-}$  (492 nm),  $S_6^{2-}$  (475 nm),  $S_4^{2-}$  (420 nm), and  $S_3^{2-}$  (270 nm). Additionally, the peak at 618 nm indicates the presence of  $S_3^{\cdot-}$  radicals. The shift in the color of the electrolyte solution to blue visually confirms the formation of  $S_3^{\cdot-}$  radicals, as shown in Figure 3D<sup>[42]</sup>. In HSEs,  $S_3^{\cdot-}$  radicals are primarily generated through the dissociation of  $S_6^{2-}$ , with minor contributions from  $S_4^{2-}$ .  $S_3^{\cdot-}$  radicals act as catalysts that promote the formation of  $S_4^{2-}$  and facilitate the conversion of  $Li_2S_4$  to  $Li_2S$ , which corresponds to the second voltage plateau. However, in lean electrolyte systems, the dissociation of  $S_6^{2-}$  into  $S_3^{\cdot-}$  radicals is inhibited and  $S_6^{2-}$  remains in its original state.

$Li_2S$ , the final discharge product, is an insulating solid that deposits on the sulfur cathode surface, leading to passivation and a decline in cathode performance over cycling. However, the high DN and typically high dielectric constant of HSEs result in significantly greater  $Li_2S$  solubility compared to SSEs. Increased  $Li_2S$  solubility reduces the deposition rate and decreases the nucleation rate, such that  $Li_2S$  growth becomes predominantly controlled by the mass transfer of short-chain LiPSs. This results in the formation of porous, spherical deposits exhibiting 3D progressive nucleation behavior. Li *et al.* analyzed the deposition behavior of  $Li_2S$  using chronoamperometric testing, applying four theoretical models that account for the kinetics of nucleation and growth processes<sup>[46]</sup>. The Bewick-Fleischman-Thirsk (BFT) models describe two-dimensional (2D) nucleation mechanisms, either progressive (2DP) or instantaneous (2DI), involving the incorporation of adatoms at the lattice interface. In contrast, the Scharifker-Hills (SH) models represent 3D nucleation, either progressive (3DP) or instantaneous (3DI), with growth controlled by volume diffusion. The key parameter distinguishing instantaneous from progressive nucleation is the nucleation rate. A high nucleation rate leads to the early depletion of nucleation sites, resulting in instantaneous growth. Conversely, when the nucleation rate is low, the density of nuclei increases linearly with time, indicative of progressive growth. After initial nucleation, subsequent growth is governed by mass transport, which may occur via surface diffusion of adatoms on the electrodeposition interface or bulk diffusion of precursors within the electrolyte. Given that the nucleation kinetics of  $Li_2S$  are influenced by the donicity of the solvent, controlling this parameter is crucial for regulating  $Li_2S$  deposition behavior<sup>[47]</sup>. As shown in Figure 3E, conventional DOL/DME electrolytes exhibit 2D nucleation, while DOL/NMP, which includes NMP with higher donicity than DME, shows a delayed transition to 3D nucleation. In contrast, DOL/NMP- $NH_4I$  electrolytes initially exhibit 3DI nucleation, followed by 3DP nucleation, confirming the occurrence of 3D  $Li_2S$  deposition. SEM images further illustrate these differences; spherical particles are more abundant in DOL/NMP- $NH_4I$ , while DOL/NMP and DOL/DME show increasingly 2D-like  $Li_2S$  deposition [Figure 3F]<sup>[43]</sup>.

Due to the severe shuttle effect, high-DN solvents such as DMSO, DMA, and N,N-dimethylformamide (DMF) have shown poor compatibility with lithium metal. Therefore, the development of high-DN solvents or additives that improve lithium metal compatibility has become a critical research focus. Zhong *et al.* investigated NMP as an additive rather than a cosolvent in HSEs, despite NMP being a high-DN solvent commonly used in such systems<sup>[44]</sup>. Figure 3G shows the SEM images and cross-sectional morphology of lithium metal in conventional DOL/DME electrolytes, while Figure 3H presents those in DOL/DME electrolytes with 1 vol% NMP as an additive. The lithium metal surface with NMP appeared significantly smoother, with no visible dendrites, and exhibited a substantial reduction in volume change in the cross-section, decreasing by approximately 56.7%. The authors attributed these improvements to a change in the SEI composition. NMP alters the Li-ion solvation structure, forming an SEI composed of inorganic components and flexible organic components, thereby improving lithium metal compatibility. Given the inherent difficulty in forming a stable SEI in HSEs, which often leads to poor lithium metal compatibility,

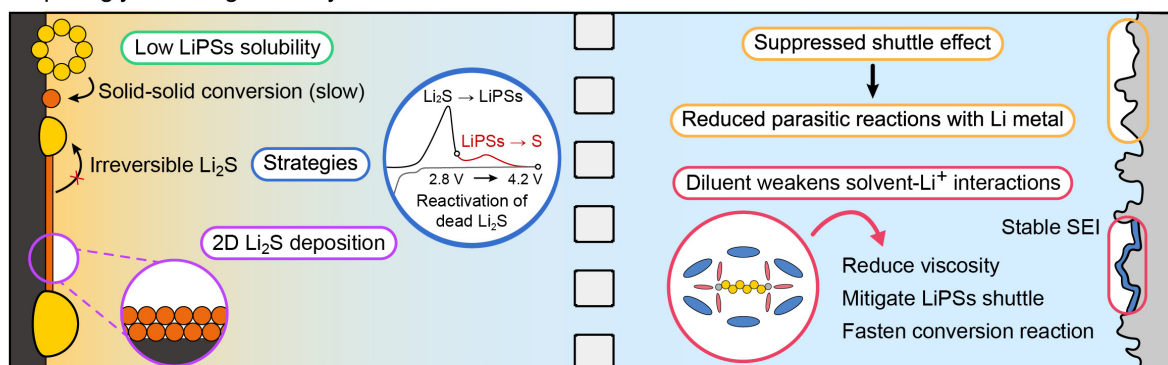
their explanation that a robust SEI improves lithium metal compatibility is highly convincing. As mentioned above, additives can be employed to modulate the composition of the SEI. Among these,  $\text{LiNO}_3$  is widely recognized as a superior additive for Li-S batteries. Due to its higher DN compared to common solvents or TFSI<sup>-</sup> anions,  $\text{LiNO}_3$  interacts more strongly with  $\text{Li}^+$ , thereby altering the solvation behavior. Its reduction results in the formation of  $\text{Li}_3\text{N}$ , a highly conductive and stable SEI component that promotes  $\text{Li}^+$  transport and enhances interfacial stability<sup>[48-50]</sup>. However, in high-DN solvents, where the solvent itself exhibits strong interactions with  $\text{Li}^+$ , the effect of  $\text{LiNO}_3$  may be diminished. Therefore, additional or alternative additive strategies may be necessary to achieve sufficient interfacial stabilization. One strategy to enhance lithium metal compatibility is the use of inherently Li-compatible high-DN solvents, which reduce the amount of free solvent molecules. Pan *et al.* reported that the incorporation of ammonium-based additives promoted the oxidation kinetics of  $\text{Li}_2\text{S}$ , thereby decreasing the concentration of free DMSO molecules and mitigating the reactivity between DMSO and lithium metal<sup>[51]</sup>. Alternatively, additives can be employed to stabilize reactive species such as  $\text{S}_3^{\cdot-}$  radicals. Pyridine (PN), another high-DN solvent, has also been explored in combination with fluorine-functionalized derivatives such as 3-fluoropyridine (3-FPN) and 4-fluoropyridine (4-FPN). Among these derivatives, 3-FPN showed superior performance by effectively stabilizing  $\text{S}_3^{\cdot-}$  radicals. This stabilization process not only enhanced the reactivity of the sulfur species but also promoted the formation of a LiF-rich SEI layer. The robust SEI significantly improved compatibility between the electrolyte and lithium metal, leading to better overall battery performance<sup>[25]</sup>.

An alternative strategy involves anchoring  $\text{S}_3^{\cdot-}$  radicals to accelerate sulfur reaction kinetics. Anchoring these radicals is essential for expediting sulfur redox reactions by driving the conversion process prior to the diffusion of LiPSs from the cathode. This mechanism effectively suppresses the shuttle effect by reducing the transport of soluble LiPSs to the anode, while simultaneously facilitating the formation of  $\text{Li}_2\text{S}$ . This is crucial for enhancing both the electrochemical performance and stability of Li-S batteries. Cui *et al.* utilized ultrathin nitrogen-oxygen co-doped carbon nanosheets (S@UN/O-CNS) as a cathode material, which effectively anchored  $\text{S}_3^{\cdot-}$  radicals through abundant N-O active sites, as evidenced by electron paramagnetic resonance (EPR) measurements [Figure 3I]<sup>[45]</sup>. EPR spectra revealed additional peaks at  $G = 2.035$  and  $G = 2.053$  with the use of UN/O-CNS, indicating the presence of  $\text{S}_3^{\cdot-}$  radicals. Furthermore, UN/O-CNS captured and catalyzed polysulfides, enhancing  $\text{Li}_2\text{S}$  deposition and dissolution. This led to accelerated reaction kinetics and shuttle effect suppression in cyclic voltammetry (CV) profiles [Figure 3J], enabling reversible sulfur redox reactions with extended cycling performance and high load capacity.

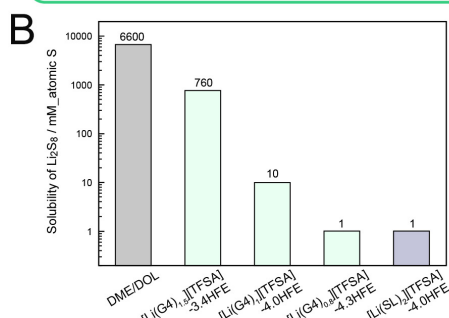
### Sparingly solvating electrolytes

SSEs typically use room-temperature ionic liquid electrolytes, which are characterized by low volatility, non-flammability, and moderate ionic conductivity. However, compared to conventional ether-based electrolytes, SSEs have lower ionic conductivity and higher viscosity, leading to significantly reduced LiPSs solubility and hindered cathode reaction kinetics. As shown in Figure 4A,  $\text{Li}_2\text{S}$  deposits in a flat 2D morphology, leading to passivation of the cathode. As cycling progresses, irreversible  $\text{Li}_2\text{S}$  tends to accumulate on the cathode, resulting in low sulfur utilization. Despite these limitations on the cathode side, the anode side demonstrates excellent stability due to the suppressed shuttle effect. To overcome these drawbacks, diluents and imide-based lithium salts are commonly used. Diluents reduce the interaction between solvent molecules and  $\text{Li}^+$  ions, thereby not significantly altering the LiPSs solubility of the electrolyte. Among imide-based salts, lithium bis (fluorosulfonyl)imide (LiFSI) is particularly effective due to its efficient decomposition and the formation of LiF, which positively impacts the surface chemistry of the lithium metal anode. Additionally, previous studies have demonstrated that using dual salts such as lithium bis (trifluoromethanesulfonyl)imide (LiTFSI)/LiFSI helps form a stable SEI<sup>[56]</sup>. When both diluents and imide-based lithium salts are used together, they effectively suppress the dissolution of soluble LiPSs and improve anode stability<sup>[57]</sup>. The most critical characteristic of SSEs, their low LiPSs solubility, results in

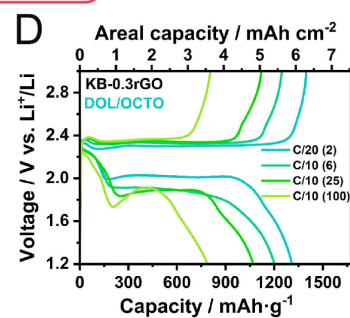
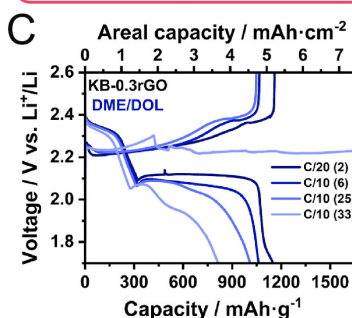
## A Springly solvating electrolytes



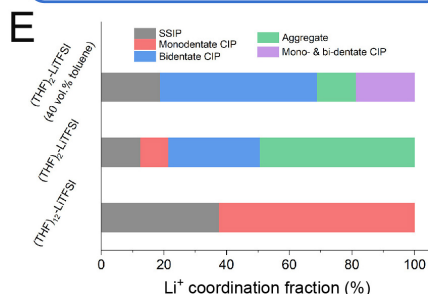
### Optimizing electrolytes for low LiPSs solubility



### Enhanced cycling stability by using the diluent



### Reducing CIP and AGG using anti-solvent



### Reactivating $\text{Li}_2\text{S}$ by increasing the cut-off voltage

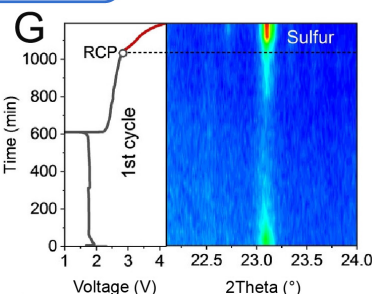
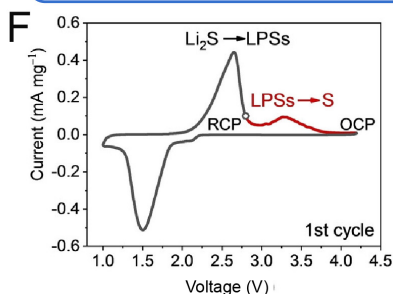


**Figure 4.** (A) Schematic of advantages and challenges of using SSEs in Li-S batteries. The figure in the blue circle is quoted and modified from Qi *et al.*<sup>[52]</sup> Copyright 2023, Wiley-VCH GmbH; (B) Saturation solubility of  $\text{Li}_2\text{S}_8$  (expressed in mM of atomic S) in the electrolytes, where  $\text{Li}_2\text{S}_8$  is the nominal formula, assuming a complete reaction between  $\text{S}_8$  and  $\text{Li}_2\text{S}$  without disproportion reactions. This figure is quoted and reproduced from Yanagi *et al.*<sup>[53]</sup> Copyright 2020, The Electrochemical Society by IOP; Charge/discharge voltage profiles evolution with cycling for cells with (C) DOL/OCTO and (D) DOL/DME electrolytes in the corresponding voltage window. These figures are quoted and reproduced from Robles-Fernández *et al.*<sup>[54]</sup> Copyright 2024, Elsevier Ltd.; (E) The calculated fraction of  $\text{Li}^+$  coordinating complexes in the electrolytes of  $(\text{THF})_{12}\text{-LiTFSI}$ ,  $(\text{THF})_2\text{-LiTFSI}$ , and  $(\text{THF})_2\text{-LiTFSI/toluene}$ . This figure is quoted and reproduced from Liu *et al.*<sup>[55]</sup> Copyright 2023, Elsevier Inc.; (F) The initial CV curve of Li-S batteries in the non-solvating  $\text{G}_{2.0.8}\text{LiTFSI}$  electrolyte (G) *In-situ* XRD of the cathode during the initial cycle with the  $\text{G}_{2.0.8}\text{LiTFSI}$  electrolyte. These figures are quoted and reproduced from Qi *et al.*<sup>[52]</sup>.

slow solid-solid conversion in the sulfur redox reaction due to the limited dissolution of soluble LiPSs on the cathode side. Furthermore, the absence of  $\text{S}_3^{\cdot-}$  radicals, which serve as crucial redox mediators in Li-S batteries, greatly impedes sulfur redox reaction kinetics in SSEs. The oxidation of  $\text{Li}_2\text{S}$  back to sulfur in SSEs requires a three-phase interface involving  $\text{Li}_2\text{S}$ , the conductive substrate, and the electrolyte. This interface enables  $\text{Li}^+$  ions from  $\text{Li}_2\text{S}$  to coordinate with solvent molecules for solvation, but the process demands a large overpotential<sup>[58]</sup>. In conventional electrolytes and HSEs, this overpotential is well within the operating voltage range, and the typical cut-off voltage of 2.8 V does not hinder the oxidation reaction. However, in

SSEs, the significantly higher overpotential required for  $\text{Li}_2\text{S}$  oxidation exceeds the 2.8 V cut-off voltage, making it insufficient to drive the reaction. This not only slows down the oxidation process but also often leads to incomplete conversion, resulting in sluggish reaction kinetics and capacity fading.

SSEs are commonly formulated using low-DN solvents or by increasing lithium salt concentrations. Figure 4B clearly illustrates this concept, showing that even with the same tetraglyme (G4) solvent, LiTFSI as a lithium salt, and Hydrofluoroether (HFE) diluent, varying their ratios results in significant differences in the solubility of  $\text{Li}_2\text{S}_8$ . The solubility of  $\text{Li}_2\text{S}_8$  was the lowest in  $[\text{Li}(\text{G4})_{0.8}][\text{TFSI}]$ , which has the smallest solvent ratio, and similarly, using the low-DN solvent SL also reduced  $\text{Li}_2\text{S}_8$  solubility<sup>[59]</sup>. Low-DN solvents exhibit weak electron-donating tendencies toward cations, making it difficult to stabilize  $\text{Li}^+$  within LiPSs, thereby restricting LiPSs formation. Alternatively, increasing lithium salt concentrations leverages the "common ion effect" to effectively lower LiPSs solubility. High concentrations of lithium salt dissociate into cations and anions, creating an environment with fewer free solvent molecules and a higher proportion of anions. This shift reduces the proportion ofSSIP structures while increasing the dominance of CIP and AGG structures in the Li-ion solvation environment. The prevalence of CIP and AGG reduces  $\text{Li}^+$  mobility, leading to decreased ionic conductivity. While this suppresses the shuttle effect and prevents lithium metal corrosion, the reduction in  $\text{Li}^+$  mobility presents a significant drawback in SSEs. In SSEs,  $\text{Li}^+$  transport transitions to a hopping mechanism, where  $\text{Li}^+$  moves between adjacent coordinating sites. For example, Pang *et al.* demonstrated this mechanism using an  $(\text{ACN})_2$ -LiTFSI complex, formed by combining all acetonitrile (ACN) molecules with LiTFSI in a 2:1 ratio<sup>[60]</sup>. This formulation eliminates free ACN molecules and reduces LiPSs solubility for anode stabilization, but the electrolyte exhibits extremely high viscosity (13.8 cP) and low ionic conductivity ( $1.35 \text{ mS cm}^{-1}$ ). These drawbacks critically hinder ion transport within the cell, posing a significant challenge for SSEs. Addressing these issues is essential for improving the performance of SSE-based Li-S batteries, as the trade-off between mitigating the shuttle effect and maintaining sufficient ionic conductivity remains a key obstacle.

To address these limitations, diluents are introduced into SSEs for optimization. HFE is commonly used as a diluent due to its low polarity, which prevents LiPSs dissolution. Additionally, HFE contributes to the formation of robust SEI layers on the anode and reduces electrolyte viscosity, thereby improving  $\text{Li}^+$  conductivity. In the  $(\text{ACN})_2$ -LiTFSI electrolyte system, the addition of HFE reduced viscosity to 8.6 cP and slightly increased ionic conductivity to  $1.57 \text{ mS cm}^{-1}$ . Notably, the solubility of LiPSs in SSEs can vary significantly depending on the ratio of solvent to diluent. Yanagi *et al.* investigated this using LiTFSI salts with G4 and HFE diluents<sup>[53]</sup>. They demonstrated that the solubility of  $\text{Li}_2\text{S}_8$  ranged from 760 mM in  $[\text{Li}(\text{G4})_{1.5}][\text{TFSI}]-3.4\text{HFE}$  (classified as HSEs) to 1 mM in  $[\text{Li}(\text{G4})_{0.8}][\text{TFSI}]-4.3\text{HFE}$  and  $[\text{Li}(\text{SL})_2][\text{TFSI}]-4.0\text{HFE}$  (classified as SSEs). In comparison, conventional DOL/DME electrolytes dissolve up to 6,600 mM of  $\text{Li}_2\text{S}_8$ , highlighting the sparingly solvating nature of SSEs. Under efficient electrolyte conditions at low current densities, both HSEs and SSEs demonstrate comparable capacity. However, SSEs, such as  $[\text{Li}(\text{G4})_1][\text{TFSI}]-4.0\text{HFE}$ , which exhibits a  $\text{Li}_2\text{S}_8$  solubility of 10 mM, showed an extremely low Li transference number ( $t_{\text{Li}^+}$ ) of 0.018, leading to severe concentration polarization and overvoltage. In contrast, cells with  $[\text{Li}(\text{SL})_2][\text{TFSI}]-4.0\text{HFE}$  showed superior rate capability due to a higher  $t_{\text{Li}^+}$ , which improved sulfur utilization. Since Li-S batteries rely more heavily on  $\text{Li}^+$  transport compared to LIB, optimizing  $t_{\text{Li}^+}$  is crucial for improving SSE performance. A novel diluent, 1H,1H,5H-octafluoropentyl-1,1,2,2-tetrafluoroethyl ether (OCTO), has recently been explored. Robles-Fernández *et al.* developed SSEs by combining DOL and OCTO (1:1 vol%) with 1.5 M LiTFSI. OCTO, an HFE-based diluent, demonstrated excellent compatibility with lithium metal<sup>[54]</sup>. Using reduced graphene oxide (rGO) sheets, they fabricated a high-sulfur loading cathode (KB-0.3rGO) that enhanced conductivity, mechanical properties, and electrode wettability. However, the cyclability of this cathode was limited in conventional DOL/DME electrolytes

[Figure 4C]. Replacing the DOL/DME electrolyte with DOL/OCTO effectively suppressed the shuttle effect, significantly improving cell durability [Figure 4D].

Recent studies have proposed the use of anti-solvents rather than diluents, as a novel strategy to improve the performance of SSEs. Liu *et al.* introduced aromatic molecules, known for their low density and cost-effectiveness, as anti-solvents<sup>[55]</sup>. Specifically, they utilized toluene to modify the electrolyte composition and observed its significant influence on Li<sup>+</sup> solvation, altering the proportions of solvation structures. For example, (THF)<sub>12</sub>-LiTFSI, which exhibits highly solvating tendencies, predominantly formed SSIP and CIP structures without the presence of AGG. In contrast, (THF)<sub>2</sub>-LiTFSI, introduced as a SSEs, demonstrated a high AGG fraction of 50% and a low SSIP fraction of only 13%. Remarkably, adding toluene at a 40% volume ratio to (THF)<sub>2</sub>-LiTFSI reduced the AGG fraction to 13% while increasing the SSIP proportion and forming more CIP structures [Figure 4E]. This adjustment resulted in decreased viscosity and improved ionic conductivity. Additionally, toluene offers advantages that go beyond the typical benefits of HFE diluents. Unlike HFEs, toluene effectively dissolves S<sub>8</sub>, promoting sulfur reactions and enhancing overall cathode kinetics. Toluene also stabilizes lithium metal, remains stable at high temperatures, and has low volatility, minimizing gas generation. By facilitating earlier Li<sub>2</sub>S nucleation, toluene addresses the critical limitation of sluggish solid-solid conversion in SSEs, enabling a quasi-solid-state reaction. As a result, the (THF)<sub>2</sub>-LiTFSI/toluene electrolyte demonstrated excellent performance, maintaining a capacity of 1,100 mAh g<sup>-1</sup> after 150 cycles at 35 °C.

One of the major challenges in SSEs is the large overpotential required for Li<sub>2</sub>S oxidation, which limits its ability to convert back to sulfur during charging. Qi *et al.* investigated this issue and attributed the poor cyclability of SSE-based cells to the accumulation of inactive Li<sub>2</sub>S, which forms large aggregates on the cathode and remains irreversibly deposited<sup>[52]</sup>. They identified this phenomenon as the primary cause of rapid capacity fade in SSEs. To address this, they defined a standard charge cut-off voltage of 2.8 V as the routine charging protocol (RCP) and evaluated its limitations. Even after replacing the lithium metal in a cell that had undergone 300 cycles and experienced significant capacity fading, no improvement in capacity was observed. This result indicates that capacity loss was primarily caused by irreversible reactions at the cathode, rather than issues at the anode. To overcome this problem, the researchers developed an optimized charging protocol (OCP), increasing the cut-off voltage from 2.8 to 4.2 V [Figure 4F]. This adjustment reactivated the dead Li<sub>2</sub>S aggregates, enabling their conversion back to sulfur and reinitiating efficient sulfur redox reactions, thereby significantly improving sulfur utilization [Figure 4G]. These findings highlight how electrochemical approaches can address the limitations of SSEs, offering new pathways to enhance their performance.

### Weakly solvating electrolytes

WSEs are characterized by intermediate properties between HSEs and SSEs. They maintain a balanced LiPSs solubility that is neither excessively high nor overly low. Proposed as an innovative electrolyte strategy, WSEs address the limitations of both HSEs and SSEs. As shown in Figure 5A, WSEs achieve an appropriate level of LiPSs solubility, which allows them to effectively suppress the shuttle effect and anode corrosion - issues commonly associated with HSEs. At the same time, WSEs mitigate drawbacks of SSEs, such as sluggish cathode kinetics, high viscosity, and low ionic conductivity. Typically, WSEs utilize solvents that are closer to low-DN solvents rather than high-DN solvents, with diluents or cosolvents added to further optimize their properties. For instance, WSEs using di-isopropyl sulfide (DIPS), a low-DN solvent, effectively limit excessive LiPSs dissolution while minimizing lithium metal corrosion, thereby ensuring stable cyclability for Li-S batteries<sup>[61]</sup>.

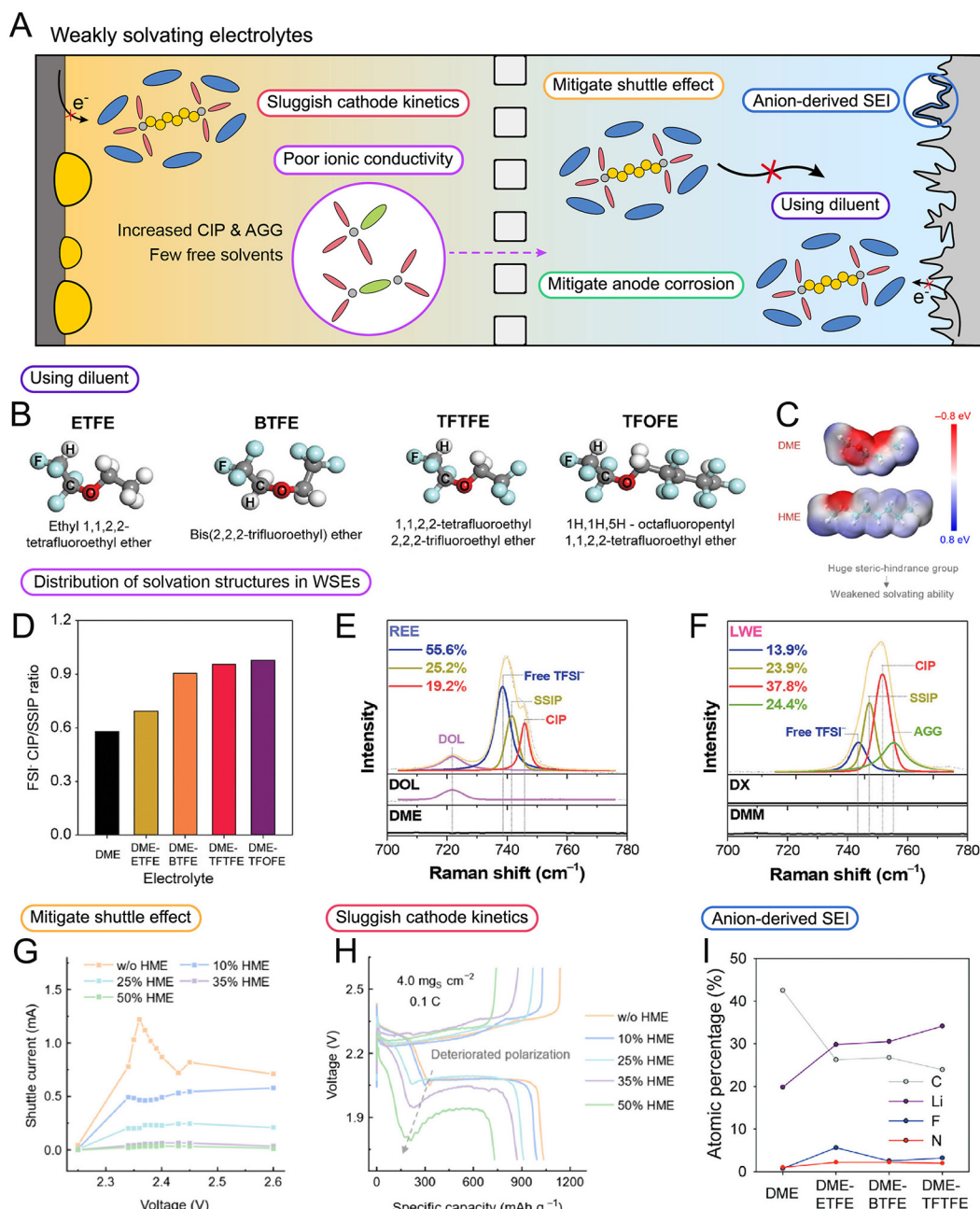


**Figure 5.** (A) Schematic of advantages and challenges of using WSEs in Li-S batteries. (B, D and I) Chemical structures of the FE cosolvents, CIP/SSIP ratio of FSI<sup>-</sup> determined via Raman analysis, and atomic compositions of the SEIs in the DME, DME-ETFE, DME-BTFE, and DME-TTFTE electrolytes after 36 cycles of operation. These figures are quoted and reproduced from Kim *et al.*<sup>[62]</sup> Copyright 2024, Wiley-VCH GmbH; (C, G and H) Electrostatic potentials of the moderately solvating solvent (DME) and weakly solvating solvent (HME) (isovalue: 0.001 a.u.), shuttle currents at various potentiostatic charging voltages, and profiles of activation polarization vs. DOD and their comparison at DOD = 0.3 (the inset figure). These figures are quoted and reproduced from Li *et al.*<sup>[63]</sup> Copyright 2024, American Chemical Society; (E and F) Raman spectra along with the distribution of free TFSI<sup>-</sup> (blue line), SSIPs (olive line), CIPs (light red line), and AGGs (green line) within the REE and LWE electrolyte systems. These figures are quoted and reproduced from Pham *et al.*<sup>[64]</sup> Copyright 2024, Wiley-VCH GmbH.

Diluents or cosolvents used in WSEs are typically selected based on their ability to reduce the Lewis basicity of electronegative atoms, such as oxygen or fluorine. This is usually achieved by incorporating molecular

structures with long, non-polar chains such as alkyl chains. Gao *et al.* investigated the impact of fluorine atoms in ether molecules on LiPSs solubility<sup>[29]</sup>. Their findings showed that as the number of fluorine atoms increased, LiPSs solubility decreased significantly. Detailed analysis revealed that both oxygen and fluorine atoms play a critical role in influencing the solubility of LiPSs. Kim *et al.* designed an electrolyte using a fluorinated ether (FE) solvent with weak solvating power toward LiPSs to achieve a balance between solubility and stability [Figure 5B]<sup>[62]</sup>. The molecular series ethyl 1,1,2,2-tetrafluoroethyl ether (ETFE), bis(2,2,2-trifluoroethyl) ether (BTFE), 1,1,2,2-tetrafluoroethyl 2,2,2-trifluoroethyl ether (TFTFE), and 1H,1H,5H-octafluoropentyl 1,1,2,2-tetrafluoroethyl ether (TFOFE) demonstrates a trend where chain length and fluorine content increase with each compound. This progression leads to greater steric hindrance, weakening the solvation ability with Li<sup>+</sup>. The increased presence of fluorine further reduces LiPSs solubility by disrupting solvation interactions. In the case of TFOFE, oxygen atoms are flanked by electron-withdrawing groups, which significantly diminish their Lewis basicity. The electron density around the oxygen atoms is reduced due to the electron-withdrawing nature of these groups, resulting in a lower overall electron density. This reduction weakens the ability of oxygen to donate electrons, thereby diminishing its Lewis basicity. As a result, the interaction between Li<sup>+</sup> and the solvent becomes the weakest among the studied molecules. This decreased interaction lowers TFOFE's ability to solvate both Li<sup>+</sup> and LiPSs effectively, making it particularly suitable for WSE formulations designed to limit LiPSs dissolution while maintaining other essential electrolyte properties. Similarly, Figure 5C demonstrates that HME, with a longer carbon chain than DME, increases steric hindrance and reduces solvation ability<sup>[63]</sup>. Ultimately, weakening Li-ion interaction is a common strategy to decrease LiPSs solubility. As Li-ion solvation weakens, structures such as CIP and AGG become more prevalent, resembling characteristics seen in SSEs. As shown in Figure 5D, the CIP/SSIP ratio increases as chain lengthens from ETFE to TFOFE, reflecting the expected decline in solvation power.

Another example involves the design of a low-concentration WSE (LWE) by mixing 1,4-dioxane (DX) and dimethoxymethane (DMM) in a 0.4 M LiTFSI<sup>[60]</sup>. In comparison, the widely used reference ether-based electrolyte (REE) for Li-S batteries consists of 1.0 M LiTFSI in DOL/DME (1:1 vol%). Raman spectroscopy analysis revealed distinct differences in solvation structures: REE exhibited abundant free solvents with no AGG, whereas LWE showed a significant increase in AGG and CIP proportions, along with a notable reduction in free solvent content [Figures 5E and F]<sup>[64]</sup>. The higher AGG and CIP ratios in WSEs can lead to issues such as increased viscosity and reduced ionic conductivity, which contribute to concentration polarization. However, a more critical challenge is the rapid increase in activation polarization. Li *et al.* investigated the cause of deteriorated cathode kinetics in WSEs with HME diluents and identified activation polarization as the primary factor<sup>[63]</sup>. While increasing HME diluent content effectively reduced LiPSs solubility and mitigated the shuttle effect, as evidenced by shuttle current measurements [Figure 5G], it also contributed to higher activation polarization. The introduction of diluents not only reduces shuttle current but also plays a significant role in controlling dendrite growth behavior. In conventional ether-based solvents, Li dendrites tend to form a mossy morphology, and prolonged cycling leads to the accumulation of large dendritic structures, which can ultimately trigger short circuits<sup>[65,66]</sup>. However, when diluents are introduced to modulate the Li<sup>+</sup> solvation structure and promote the formation of anion-derived SEI layers, a more stable SEI is formed, resulting in uniform Li deposition and effectively mitigating dendrite formation. Nevertheless, the use of diluents may lower reaction kinetics and increase activation polarization, which could become a critical factor leading to the failure of WSEs. To address this issue, TiN nanoparticles were introduced as LiPSs electrocatalysts to enhance the redox kinetics of polysulfides and support stable electrochemical performance. As a result, the use of TiN electrocatalysts substantially mitigated activation polarization, as shown in Figure 5H. In addition to enhancing cathode kinetics, strategies for forming a stable SEI have also been explored to ensure lithium metal stability. Research on DME-FE electrolytes, in which FE was used as a cosolvent, aimed to reduce carbon content and promote the formation of inorganic

SEIs enriched with Li, N, and F. The weak solvation power in these electrolytes facilitated the formation of such SEIs, which in turn effectively suppressed lithium metal corrosion [Figure 5].

### Summary of electrolyte concepts and challenges

The electrolyte strategies discussed above have led to improvements in the performance of Li-S batteries by tuning the properties of solvents and additives. Table 1 summarizes the components introduced in each strategy and their corresponding electrochemical performance. In the case of HSEs, their strong chemical affinity toward polysulfides enables excellent reaction kinetics, resulting in high specific capacity. However, this also increases the reactivity between polysulfides and the lithium metal anode, leading to rapid capacity fading and poor stability. To mitigate issues arising from the presence of large quantities of polysulfides, the use of functional separators that prevent polysulfide crossover to the anode side can be an effective solution<sup>[67,68]</sup>. Additionally, functional nano-carbon-based cathodes that encapsulate sulfur can not only buffer sulfur's volume expansion but also suppress direct contact with HSEs, thereby reducing excessive polysulfide dissolution SSEs, due to their extremely low polysulfide solubility, provide excellent anode stability and low interfacial resistance between the anode and electrolyte<sup>[69,70]</sup>. However, achieving sufficient capacity with SSEs remains challenging. To address this, it is necessary to develop high-capacity cathodes compatible with SSEs or to incorporate catalytic materials that enhance reaction kinetics. In WSEs, a moderate level of polysulfide solubility enables minimal reactivity with the lithium metal anode while maintaining sufficient polysulfides for electrochemical operation. However, their performance is highly dependent on the content of the weakly solvating solvent, meaning that auxiliary strategies such as catalyst incorporation, similar to those used in SSE systems, may be required<sup>[71,72]</sup>.

The electrolyte strategies evaluated in this study highlight the importance of balancing sulfur redox kinetics and lithium metal stability to realize high-performance Li-S batteries. Achieving high specific capacity requires sufficient polysulfide solubility; however, excessive local concentrations of dissolved polysulfides can lead to uneven corrosion and compromised interfacial stability at the anode. Therefore, controlling the dissolution behavior of polysulfides is essential. Furthermore, the lithium metal anode exhibits high reactivity and is typically paired with volatile and flammable organic electrolytes, raising safety concerns. Therefore, in addition to developing flame-retardant electrolyte systems, the use of flame-retardant cathodes such as sulfurized polyacrylonitrile (SPAN), which possess low limited oxygen index (LOI) values, should be actively considered<sup>[73,74]</sup>. As electrolyte reduction directly contributes to SEI formation, it significantly influences dendrite growth, a leading cause of short circuits. To promote the formation of stable anion-derived SEI and enhance lithium reversibility, the reduction potential gap between the electrolyte anion and Li/Li<sup>+</sup> must be sufficiently large. Moreover, to improve oxidation stability, additives with lowest unoccupied molecular orbital (LUMO) levels higher than those of the solvents should be employed to preferentially undergo reduction and contribute to SEI stabilization<sup>[75,76]</sup>.

## CONCLUSION AND OUTLOOK

Designing electrolytes that regulate the solubility and behavior of LiPSs is crucial for achieving high-performance Li-S batteries. Depending on the solubility of LiPSs, critical cell-level parameters such as conversion kinetics, shuttle effect severity, Li<sub>2</sub>S deposition morphology, and lithium metal stability can vary significantly [Figure 6]. While LiPSs facilitate the conversion from S<sub>8</sub> to Li<sub>2</sub>S, excessive dissolution exacerbates the shuttle effect, leading to side reactions such as self-discharge and lithium metal corrosion. When solvent molecules interact strongly with LiPSs, Li<sub>2</sub>S tends to deposit in a 3D morphology, which enhances cathode kinetics but can cause passivation when deposited on the lithium metal surface due to its poor electronic conductivity. To address these complexities, electrolyte systems for Li-S batteries are broadly categorized into three types - HSEs, SSEs, and WSEs - based on LiPSs solubility, with each category having distinct design strategies.

**Table 1. A summary of electrolyte strategy components and corresponding electrochemical performance**

Type of electrolyte	Electrolyte	E/S ratio	Cathode/S loading (mg <sub>s</sub> cm <sup>-2</sup> )	C-rate	Initial discharge capacity (mAh g <sup>-1</sup> )	Discharge capacity (mAh g <sup>-1</sup> )	Capacity retention	Ref.
HSE	1 M LiTFSI in 3-FPN	7	S@C/1	0.1	1,087.9 (at 0.03 C)	792.7 (100 cycles)	72.6% at 100 cycles	[25]
HSE	1 M LiTFSI in DOL/DME (1:1 vol%) + 0.3 M LiNO <sub>3</sub> , 0.1 M FL	8	S@PC	0.2	908	760.9 (100 cycles)	-	[41]
HSE	1 M LiTFSI in DOL/DME (1:1 vol%) + 2 wt% LiNO <sub>3</sub> , 0.1 M T3Br	10	S@KB/4.6	0.1	883	855 (100 cycles)	-	[42]
HSE	0.8 M LiTFSI in DOL/NMP (1:1 vol%) + 0.2 M LiNO <sub>3</sub> , 0.1 M NH <sub>4</sub> I	5	S@CNT	0.1	1092	-340 (50 cycles)	-	[43]
HSE	1 M LiTFSI in DOL/DME (1:1 vol%) + 2 wt% LiNO <sub>3</sub> , 1 vol% NMP	15	S@KB	0.3	1,250 (at 0.05 C)	800 (100 cycles)	-	[44]
HSE	1 M LiTFSI in DOL/DME (1:1 vol%) + 2 wt% LiNO <sub>3</sub>	-	S@UN/O-CNS	0.5	-1,050	-800 (100 cycles)	-	[45]
SSE	G <sub>2.0.8</sub> LiTFSI to TTE (1:2 vol%)	-	S@KB/1	0.2	-	-1,400 (100 cycles, OCP method)	-	[52]
SSE	1 M [Li(G <sub>4</sub> ) <sub>0.8</sub> ][TFSI]-4.3HFE in DOL/DME (1:1 vol%) + 0.2 M LiNO <sub>3</sub>	10	S@C/3	0.02 discharge/0.01 charge	1,100	-	-	[53]
SSE	1 M [Li(SL) <sub>2</sub> ][TFSI]-4.0HFE in DOL/DME (1:1 vol%) + 0.2 M LiNO <sub>3</sub>	10	S@C/3	0.02 discharge/0.01 charge	1,200	-	-	[53]
SSE	1.5 M LiTFSI in DOL/OCTO (1:1 vol%) + 0.5 M LiNO <sub>3</sub>	7	S@KB-rGO/4.5	0.1	1,200	780 (100 cycles)	-	[54]
SSE	(THF) <sub>2</sub> -LiTFSI/hydrofluoroether	20	S@KB/1	0.1	-1,270	-850 (100 cycles)	-	[55]
SSE	(THF) <sub>2</sub> -LiTFSI/Toluene	20	S@KB/1	0.1	-1,350	-1,100 (100 cycles)	-	[55]
WSE	LiFSI:LiNO <sub>3</sub> :DME:ETFE = 1.9:1.0:18.5:3.8 (molar ratio)	5	S-loaded electrode/3.8	0.15	-	-	70% at 32 cycles	[62]
WSE	LiFSI:LiNO <sub>3</sub> :DME:BTFE = 1.9:1.0:18.5:3.8 (molar ratio)	5	S-loaded electrode/3.8	0.15	-	-	70% at 131 cycles	[62]
WSE	LiFSI:LiNO <sub>3</sub> :DME:TFTFE = 1.9:1.0:18.5:3.8 (molar ratio)	5	S-loaded electrode/3.8	0.15	-	-	70% at 154 cycles	[62]
WSE	LiFSI:LiNO <sub>3</sub> :DME:TFOFE = 1.9:1.0:18.5:3.8 (molar ratio)	5	S-loaded electrode/3.8	0.15	-	-	70% at 31 cycles	[62]
WSE	1 M LiTFSI in DOL/DME (1:1 vol%) + 35 vol% HME + 2 wt% LiNO <sub>3</sub>	11.25	S@CNT/4	0.1	-	1,200 (100 cycles, with TiN electrocatalyst)	-	[63]
WSE	0.4 M LiTFSI in 1,4-DX/DMM	-	SPAN	0.3	671	-470 (100 cycles)	70% at 100 cycles	[64]

PC: Porous carbon; KB: ketjen black.

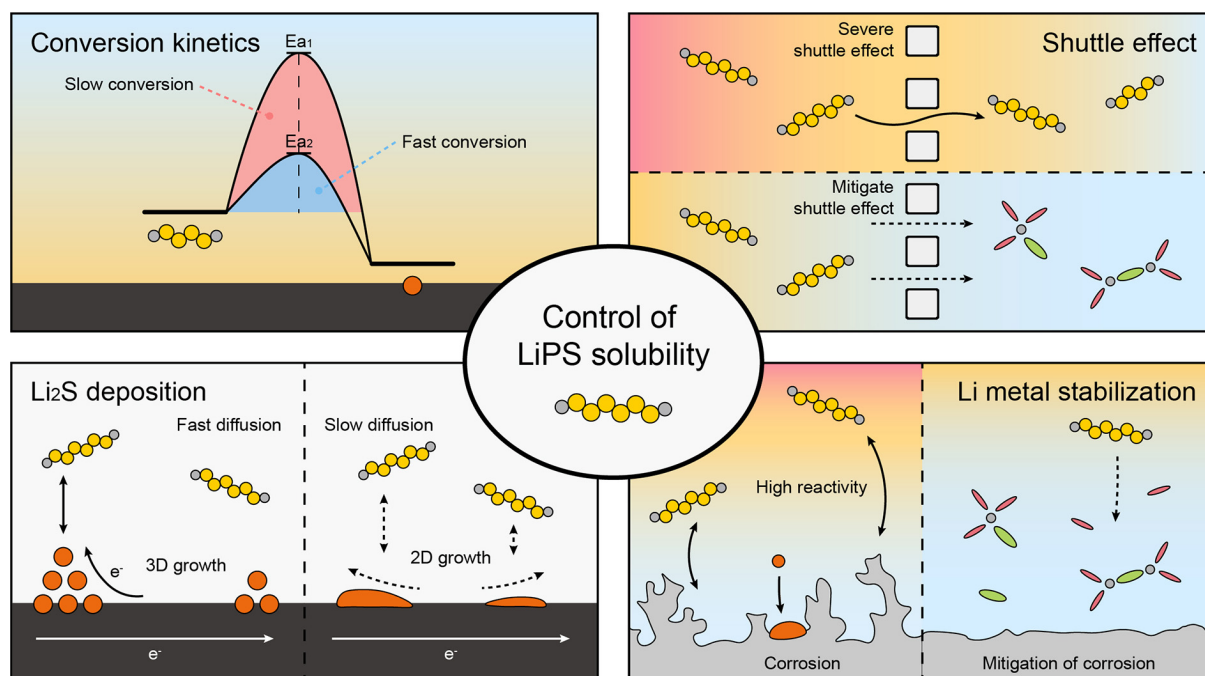


**Figure 6.** Schematic of controlling LiPSs solubility to regulate key aspects of Li-S batteries, including conversion kinetics, shuttle effect, Li<sub>2</sub>S deposition, and lithium metal stabilization.

HSEs provide high polysulfide solubility and enable fast redox kinetics through the stabilization of  $S_3^{\cdot-}$  radicals. However, they suffer from severe shuttle effects, lithium metal passivation, and corrosion. To address these challenges, further research is needed on additives, functional carbon composites, and separators that are compatible with high-DN solvents while suppressing excessive polysulfide dissolution. SSEs significantly suppress polysulfide dissolution, thereby stabilizing the lithium metal. However, they face major limitations such as sluggish cathode kinetics, low ionic conductivity, and high viscosity, leading to short cycle life. To overcome these drawbacks, low-viscosity diluents and anti-solvent concepts have been introduced. WSEs aim to balance polysulfide solubility to enhance cathode kinetics while suppressing parasitic reactions. These systems employ various diluents to promote the formation of stable SEI layers and enhance interfacial stability on the lithium metal. To further facilitate sulfur redox reactions, additional electrocatalysts are required. Recently, moderately solvating electrolytes with slightly higher polysulfide solubility than conventional WSEs have been proposed to improve cathode kinetics while maintaining adequate protection for the anode. In conclusion, each electrolyte strategy offers distinct advantages and addresses different aspects of battery performance.

Further progress beyond electrolyte optimization is required for the commercialization of Li-S batteries. In practical applications, lean electrolyte configurations are essential for maximizing gravimetric energy density. Under such conditions, where the electrolyte volume is minimized, achieving high specific capacity requires a sufficiently high polysulfide concentration<sup>[77,78]</sup>. Additionally, a uniform concentration gradient must be maintained throughout the cell to ensure homogeneous reaction kinetics. Considering these aspects, future electrolyte systems must be designed to form a stable interface at the anode while maintaining favorable chemical compatibility with sulfur at the cathode.

Several challenges remain to be addressed before commercialization, extending beyond the goal of improving energy density. One of the primary issues is the commercial viability of the proposed electrolyte systems. The electrolyte accounts for a significant portion of the overall cost in Li-S batteries. Lithium salts such as LiTFSI and LiFSI, commonly used in electrolytes, are expensive and contribute substantially to the total cost. To address this, studies have focused on reducing the use of commercially available fluorine-based lithium salts<sup>[79]</sup>. In addition, solvents frequently used as diluents are costly and have limited production volumes, posing a challenge for large-scale application. To overcome these limitations, developing low-cost and environmentally friendly ether-based diluents is essential<sup>[80]</sup>. Improvements in manufacturing processes are necessary to reduce the overall battery production costs. Another issue that has recently gained attention is battery recycling. Most electrolytes are highly volatile, flammable, and toxic, raising concerns related to environmental pollution and safety hazards such as explosions. Due to these physicochemical characteristics, recovering electrolytes is extremely difficult, making them more challenging to recycle than other battery components<sup>[81,82]</sup>. While previous research has explored methods to recycle inactive lithium using redox precursors such as 2-aminophenylacetonitrile (APA), practical recovery and reuse of organic electrolytes in Li-S batteries have yet to be demonstrated<sup>[83]</sup>.

Ultimately, no single electrolyte strategy can address all performance requirements and operational constraints. Future electrolyte systems must balance sulfur redox kinetics with lithium metal stability, facilitate uniform polysulfide utilization, minimize parasitic reactions, and form robust SEI layers at the interface. Beyond achieving high performance, continued efforts are necessary to design electrolytes that also account for practical manufacturing processes and long-term sustainability.

## DECLARATIONS

### Authors' contributions

Conceived the review and wrote the manuscript, collectively discussed and revised the manuscript: Jung, S. Y.; Yu, S. H.

Designed and drew the figures: Jung, S. Y.

Assisted in the writing of the manuscript: Park, J. Y.

### Availability of data and materials

Not applicable.

### Financial support and sponsorship

This work was supported by the National Research Foundation of Korea (NRF) grant funded by the Korean government (MSIT) (RS-2024-00455177).

### Conflicts of interest

All authors declared that there are no conflicts of interest.

### Ethical approval and consent to participate

Not applicable.

### Consent for publication

Not applicable.

### Copyright

© The Author(s) 2025.

## REFERENCES

1. Winter, M.; Brodd, R. J. What are batteries, fuel cells, and supercapacitors? *Chem. Rev.* **2004**, *104*, 4245-69. DOI PubMed
2. Whittingham, M. S. Lithium batteries and cathode materials. *Chem. Rev.* **2004**, *104*, 4271-301. DOI PubMed
3. Cano, Z. P.; Banham, D.; Ye, S.; et al. Batteries and fuel cells for emerging electric vehicle markets. *Nat. Energy.* **2018**, *3*, 279-89. DOI
4. Choi, N. S.; Chen, Z.; Freunberger, S. A.; et al. Challenges facing lithium batteries and electrical double-layer capacitors. *Angew. Chem. Int. Ed.* **2012**, *51*, 9994-10024. DOI
5. Goodenough, J. B. Electrochemical energy storage in a sustainable modern society. *Energy. Environ. Sci.* **2014**, *7*, 14-8. DOI
6. Manthiram, A.; Chung, S. H.; Zu, C. Lithium-sulfur batteries: progress and prospects. *Adv. Mater.* **2015**, *27*, 1980-2006. DOI PubMed
7. Cho, B. K.; Jung, S. Y.; Park, S. J.; Hyun, J. H.; Yu, S. H. *In Situ/Operando* imaging techniques for next-generation battery analysis. *ACS. Energy. Lett.* **2024**, *9*, 4068-92. DOI
8. Kim, J. H.; Kim, M.; Kim, S. J.; et al. Understanding the electrochemical processes of SeS<sub>2</sub> positive electrodes for developing high-performance non-aqueous lithium sulfur batteries. *Nat. Commun.* **2024**, *15*, 7669. DOI PubMed PMC
9. Wujcik, K. H.; Wang, D. R.; Raghunathan, A.; et al. Lithium polysulfide radical anions in ether-based solvents. *J. Phys. Chem. C.* **2016**, *120*, 18403-10. DOI
10. Zhang, J.; Fu, Q.; Li, P.; et al. Lithium polysulfide solvation and speciation in the aprotic lithium-sulfur batteries. *Particuology* **2024**, *89*, 238-45. DOI
11. Chen, X.; Hou, T.; Persson, K. A.; Zhang, Q. Combining theory and experiment in lithium-sulfur batteries: Current progress and future perspectives. *Mater. Today.* **2019**, *22*, 142-58. DOI
12. Kim, M.; Choi, H.; Yu, S. Recent progress in design strategies for high-performance metal-tellurium batteries. *Chem. Eng. J.* **2025**, *504*, 158528. DOI
13. Qiu, Y.; Zuo, X.; Fu, L.; Liu, D.; Zhang, Y. Design and optimization of multicomponent electrolytes for lithium-sulfur battery: a machine learning concept and outlook. *ChemCatChem* **2024**, *16*, e202400754. DOI
14. Zheng, J.; Fan, X.; Ji, G.; et al. Manipulating electrolyte and solid electrolyte interphase to enable safe and efficient Li-S batteries. *Nano. Energy.* **2018**, *50*, 431-40. DOI
15. Li, J.; Gao, L.; Pan, F.; et al. Engineering strategies for suppressing the shuttle effect in lithium-sulfur batteries. *Nanomicro. Lett.* **2023**, *16*, 12. DOI PubMed PMC
16. He, X.; Bresser, D.; Passerini, S.; et al. The passivity of lithium electrodes in liquid electrolytes for secondary batteries. *Nat. Rev. Mater.* **2021**, *6*, 1036-52. DOI
17. Deng, Z.; Jia, Y.; Deng, Y.; et al. Coordination structure regulation in non-flammable electrolyte enabling high voltage lithium electrochemistry. *J. Energy. Chem.* **2024**, *96*, 282-90. DOI
18. Kong, L.; Yin, L.; Xu, F.; et al. Electrolyte solvation chemistry for lithium-sulfur batteries with electrolyte-lean conditions. *J. Energy. Chem.* **2021**, *55*, 80-91. DOI
19. Shen, C.; Xie, J.; Zhang, M.; et al. Self-discharge behavior of lithium-sulfur batteries at different electrolyte/sulfur ratios. *J. Electrochem. Soc.* **2019**, *166*, A5287-94. DOI
20. Ye, H.; Li, Y. Towards practical lean-electrolyte Li-S batteries: highly solvating electrolytes or sparingly solvating electrolytes? *Nano. Res. Energy.* **2022**, *1*, e9120012. DOI
21. Chen, J.; Fu, Y.; Guo, J. Development of electrolytes under lean condition in lithium-sulfur batteries. *Adv. Mater.* **2024**, *36*, e2401263. DOI
22. Gupta, A.; Bhargav, A.; Jones, J. P.; Bugga, R. V.; Manthiram, A. Influence of lithium polysulfide clustering on the kinetics of electrochemical conversion in lithium-sulfur batteries. *Chem. Mater.* **2020**, *32*, 2070-7. DOI PubMed PMC
23. Gupta, A.; Bhargav, A.; Manthiram, A. Highly solvating electrolytes for lithium-sulfur batteries. *Adv. Energy. Mater.* **2019**, *9*, 1803096. DOI PubMed PMC
24. He, M.; Ozoemena, K. I.; Aurbach, D.; Pang, Q. Developing highly solvating electrolyte solutions for lithium-sulfur batteries. *Curr. Opin. Electrochem.* **2023**, *39*, 101285. DOI
25. Elabd, A.; Kim, J.; Sethio, D.; et al. Dual functional high donor electrolytes for lithium-sulfur batteries under lithium nitrate free and lean electrolyte conditions. *ACS. Energy. Lett.* **2022**, *7*, 2459-68. DOI
26. Cheng, L.; Curtiss, L. A.; Zavadil, K. R.; Gewirth, A. A.; Shao, Y.; Gallagher, K. G. Sparingly solvating electrolytes for high energy density lithium-sulfur batteries. *ACS. Energy. Lett.* **2016**, *1*, 503-9. DOI
27. Jiang, R.; Qi, X.; Ji, J.; et al. Accelerated Li<sub>2</sub>S conversion in sparingly-solvating electrolytes enabled with dipole-dipole interaction for wide-temperature Li-S batteries. *Energy. Storage. Mater.* **2024**, *66*, 103215. DOI
28. Choi, J.; Jeong, H.; Jang, J.; et al. Weakly solvating solution enables chemical prelithiation of graphite-SiO<sub>x</sub> anodes for high-energy Li-ion batteries. *J. Am. Chem. Soc.* **2021**, *143*, 9169-76. DOI
29. Gao, X.; Yu, Z.; Wang, J.; et al. Electrolytes with moderate lithium polysulfide solubility for high-performance long-calendar-life lithium-sulfur batteries. *Proc. Natl. Acad. Sci. USA.* **2023**, *120*, e2301260120. DOI PubMed PMC
30. Zhang, S. S. Liquid electrolyte lithium/sulfur battery: fundamental chemistry, problems, and solutions. *J. Power. Sources.* **2013**, *231*, 153-62. DOI

31. Kim, S. C.; Gao, X.; Liao, S. L.; et al. Solvation-property relationship of lithium-sulphur battery electrolytes. *Nat. Commun.* **2024**, *15*, 1268. DOI PubMed PMC
32. Cheng, H.; Sun, Q.; Li, L.; et al. Emerging era of electrolyte solvation structure and interfacial model in batteries. *ACS. Energy. Lett.* **2022**, *7*, 490-513. DOI
33. Nanda, S.; Bhargav, A.; Manthiram, A. Anode-free, lean-electrolyte lithium-sulfur batteries enabled by tellurium-stabilized lithium deposition. *Joule* **2020**, *4*, 1121-35. DOI
34. Zhao, J. J.; Chen, Z. X.; Cheng, Q.; et al. Electrocatalysts work better in lean-electrolyte lithium-sulfur batteries. *J. Mater. Chem. A.* **2024**, *12*, 21845-52. DOI
35. Hall, D. S.; Self, J.; Dahn, J. R. Dielectric constants for quantum chemistry and Li-ion batteries: solvent blends of ethylene carbonate and ethyl methyl carbonate. *J. Phys. Chem. C.* **2015**, *119*, 22322-30. DOI
36. Zhang, G.; Peng, H. J.; Zhao, C. Z.; et al. The radical pathway based on a lithium-metal-compatible high-dielectric electrolyte for lithium-sulfur batteries. *Angew. Chem. Int. Ed.* **2018**, *57*, 16732-6. DOI
37. Cuisinier, M.; Hart, C.; Balasubramanian, M.; Garsuch, A.; Nazar, L. F. Radical or not radical: revisiting lithium-sulfur electrochemistry in nonaqueous electrolytes. *Adv. Energy. Mater.* **2015**, *5*, 1401801. DOI
38. Gutmann, V. Empirical parameters for donor and acceptor properties of solvents. *Electrochim. Acta.* **1976**, *21*, 661-70. DOI
39. Zhou, P.; Xiang, Y.; Liu, K. Understanding and applying the donor number of electrolytes in lithium metal batteries. *Energy. Environ. Sci.* **2024**, *17*, 8057-77. DOI
40. Baek, M.; Shin, H.; Char, K.; Choi, J. W. New high donor electrolyte for lithium-sulfur batteries. *Adv. Mater.* **2020**, *32*, e2005022. DOI PubMed
41. Shen, Z.; Gao, Q.; Zhu, X.; et al. In-situ free radical supplement strategy for improving the redox kinetics of Li-S batteries. *Energy. Storage. Mater.* **2023**, *57*, 299-307. DOI
42. Meng, R.; He, X.; Ong, S. J. H.; et al. A radical pathway and stabilized Li anode enabled by halide quaternary ammonium electrolyte additives for lithium-sulfur batteries. *Angew. Chem. Int. Ed.* **2023**, *62*, e202309046. DOI
43. Shi, Z.; Thomas, S.; Tian, Z.; et al. A tailored highly solvating electrolyte toward ultra lean-electrolyte Li-S batteries. *Nano. Res. Energy.* **2024**, *3*, e9120126. DOI
44. Zhong, N.; Lei, C.; Meng, R.; Li, J.; He, X.; Liang, X. Electrolyte solvation chemistry for the solution of high-donor-number solvent for stable Li-S batteries. *Small* **2022**, *18*, e2200046. DOI
45. Cui, Y.; Fang, W.; Zhang, J.; et al. Controllable sulfur redox multi-pathway reactions regulated by metal-free electrocatalysts anchored with LiS<sub>3</sub>\* radicals. *Nano. Energy.* **2024**, *122*, 109343. DOI
46. Li, Z.; Zhou, Y.; Wang, Y.; Lu, Y. Solvent-mediated Li<sub>2</sub>S electrodeposition: a critical manipulator in lithium-sulfur batteries. *Adv. Energy. Mater.* **2019**, *9*, 1802207. DOI
47. Zhou, S.; Shi, J.; Liu, S.; et al. Visualizing interfacial collective reaction behaviour of Li-S batteries. *Nature* **2023**, *621*, 75-81. DOI
48. Li, X.; Zhao, R.; Fu, Y.; Manthiram, A. Nitrate additives for lithium batteries: mechanisms, applications, and prospects. *eScience* **2021**, *1*, 108-23. DOI
49. Zhang, X. Q.; Chen, X.; Cheng, X. B.; et al. Highly stable lithium metal batteries enabled by regulating the solvation of lithium ions in nonaqueous electrolytes. *Angew. Chem. Int. Ed.* **2018**, *57*, 5301-5. DOI
50. Um, J. H.; Yu, S. H. Unraveling the mechanisms of lithium metal plating/stripping via in situ/operando analytical techniques. *Adv. Energy. Mater.* **2021**, *11*, 2003004. DOI
51. Pan, H.; Han, K. S.; Vijayakumar, M.; et al. Ammonium additives to dissolve lithium sulfide through hydrogen binding for high-energy lithium-sulfur batteries. *ACS. Appl. Mater. Interfaces.* **2017**, *9*, 4290-5. DOI
52. Qi, X.; Yang, F.; Sang, P.; et al. Electrochemical reactivation of dead Li<sub>2</sub>S for Li-S batteries in non-solvating electrolytes. *Angew. Chem. Int. Ed.* **2023**, *62*, e202218803. DOI
53. Yanagi, M.; Ueno, K.; Ando, A.; et al. Effects of polysulfide solubility and Li ion transport on performance of Li-S batteries using sparingly solvating electrolytes. *J. Electrochem. Soc.* **2020**, *167*, 070531. DOI
54. Robles-Fernández, A.; Moreno-Fernández, G.; Soria-Fernández, A.; Castillo, J.; Santiago, A.; Carriazo, D. Towards practical Li-S batteries through the combination of a nanostructured graphene composite cathode and a novel sparingly solvating electrolyte. *Carbon* **2024**, *229*, 119442. DOI
55. Liu, Y.; Xu, L.; Yu, Y.; et al. Stabilized Li-S batteries with anti-solvent-tamed quasi-solid-state reaction. *Joule* **2023**, *7*, 2074-91. DOI
56. Liu, J.; Ghosh, A.; Kondou, S.; et al. Localized high-concentration binary salt electrolytes with suppressed Li<sub>2</sub>S<sub>x</sub> solubility to achieve stable Li-S pouch cells with high sulfur-loading cathodes under lean electrolyte conditions. *ACS. Appl. Energy. Mater.* **2025**, *8*, 1570-9. DOI
57. Castillo, J.; Soria-Fernández, A.; Rodríguez-Peña, S.; et al. Graphene-based sulfur cathodes and dual salt-based sparingly solvating electrolytes: a perfect marriage for high performing, safe, and long cycle life lithium-sulfur prototype batteries. *Adv. Energy. Mater.* **2024**, *14*, 2302378. DOI
58. Fan, F. Y.; Carter, W. C.; Chiang, Y. M. Mechanism and kinetics of Li<sub>2</sub>S precipitation in lithium-sulfur batteries. *Adv. Mater.* **2015**, *27*, 5203-9. DOI PubMed
59. Nakanishi, A.; Ueno, K.; Watanabe, D.; et al. Sulfolane-based highly concentrated electrolytes of lithium bis(trifluoromethanesulfonyl)amide: ionic transport, Li-ion coordination, and Li-S battery performance. *J. Phys. Chem. C.* **2019**, *123*, 14229-38. DOI

60. Pang, Q.; Shyamsunder, A.; Narayanan, B.; Kwok, C. Y.; Curtiss, L. A.; Nazar, L. F. Tuning the electrolyte network structure to invoke quasi-solid state sulfur conversion and suppress lithium dendrite formation in Li-S batteries. *Nat. Energy*. **2018**, *3*, 783-91. DOI
61. Hou, L. P.; Zhang, X. Q.; Yao, N.; et al. An encapsulating lithium-polysulfide electrolyte for practical lithium-sulfur batteries. *Chem* **2022**, *8*, 1083-98. DOI
62. Kim, I.; Kim, S.; Cho, H.; et al. Moderately solvating electrolyte with fluorinated cosolvents for lean-electrolyte Li-S batteries. *Adv. Energy Mater.* **2025**, *15*, 2403828. DOI
63. Li, X. Y.; Feng, S.; Song, Y. W.; et al. Kinetic evaluation on lithium polysulfide in weakly solvating electrolyte toward practical lithium-sulfur batteries. *J. Am. Chem. Soc.* **2024**, *146*, 14754-64. DOI
64. Pham, T. D.; Bin, F. A.; Kim, J.; Ma, S. H.; Kwak, K.; Lee, K. K. High-efficiency lithium metal stabilization and polysulfide suppression in Li-S battery enabled by weakly solvating solvent. *Small* **2024**, *20*, e2307951. DOI PubMed
65. Gao, X.; Zhou, Y. N.; Han, D.; et al. Thermodynamic understanding of Li-dendrite formation. *Joule* **2020**, *4*, 1864-79. DOI
66. Zhao, Y.; Zhou, T.; Ashirov, T.; et al. Fluorinated ether electrolyte with controlled solvation structure for high voltage lithium metal batteries. *Nat. Commun.* **2022**, *13*, 2575. DOI PubMed PMC
67. He, J.; Li, X. Recent materials development for Li-ion and Li-S battery separators. *J. Energy Storage*. **2025**, *112*, 115541. DOI
68. Li, Z.; Wang, J.; Yuan, H.; Yu, Y.; Tan, Y. Recent progress and challenge in metal-organic frameworks for lithium-sulfur battery separators. *Adv. Funct. Mater.* **2024**, *34*, 2405890. DOI
69. Chen, R.; Zhou, Y.; Li, X. Nanocarbon-enabled mitigation of sulfur expansion in lithium-sulfur batteries. *Energy Storage Mater.* **2024**, *68*, 103353. DOI
70. Chen, X. R.; Yu, X. F.; He, B.; Li, W. C. Encapsulation of sulfur inside micro-nano carbon/molybdenum carbide by in-situ chemical transformation for high-performance Li-S batteries. *New Carbon Mater.* **2023**, *38*, 337-44. DOI
71. Kong, X.; Kong, Y.; Zheng, Y.; He, L.; Wang, D.; Zhao, Y. Hydrofluoroether diluted dual-salts-based electrolytes for lithium-sulfur batteries with enhanced lithium anode protection. *Small* **2022**, *18*, e2205017. DOI
72. Zheng, J.; Ji, G.; Fan, X.; et al. High-fluorinated electrolytes for Li-S batteries. *Adv. Energy Mater.* **2019**, *9*, 1803774. DOI
73. Wang, J.; Lin, F.; Jia, H.; Yang, J.; Monroe, C. W.; NuLi, Y. Towards a safe lithium-sulfur battery with a flame-inhibiting electrolyte and a sulfur-based composite cathode. *Angew. Chem. Int. Ed.* **2014**, *53*, 10099-104. DOI
74. Chen, S.; Zheng, J.; Yu, L.; et al. High-efficiency lithium metal batteries with fire-retardant electrolytes. *Joule* **2018**, *2*, 1548-58. DOI
75. Zheng, B.; He, Z.; Lei, X.; Zhang, J. Microscopic insights into effects of sulfolane additive on Li-S battery electrolyte. *J. Mol. Liq.* **2024**, *413*, 126000. DOI
76. Zhao, Y.; Zhou, T.; Mensi, M.; Choi, J. W.; Coskun, A. Electrolyte engineering via ether solvent fluorination for developing stable non-aqueous lithium metal batteries. *Nat. Commun.* **2023**, *14*, 299. DOI PubMed PMC
77. Zhao, M.; Li, B. Q.; Zhang, X. Q.; Huang, J. Q.; Zhang, Q. A perspective toward practical lithium-sulfur batteries. *ACS. Cent. Sci.* **2020**, *6*, 1095-104. DOI PubMed PMC
78. Song, X.; Liang, X.; Kim, H.; Sun, Y. Practical lithium-sulfur batteries: beyond the conventional electrolyte concentration. *ACS. Energy Lett.* **2024**, *9*, 5576-86. DOI
79. Agostini, M.; Lim, D. H.; Sadd, M.; et al. Rational design of low cost and high energy lithium batteries through tailored fluorine-free electrolyte and nanostructured S/C composite. *ChemSusChem* **2018**, *11*, 2981-6. DOI
80. Kong, X.; Zheng, Y.; He, L.; Wang, D.; Zhao, Y. Butyl ether as Co-diluent in medium-concentrated electrolyte for Li-S battery. *J. Energy Chem.* **2023**, *85*, 343-7. DOI
81. Niu, B.; Xu, Z.; Xiao, J.; Qin, Y. Recycling hazardous and valuable electrolyte in spent lithium-ion batteries: urgency, progress, challenge, and viable approach. *Chem. Rev.* **2023**, *123*, 8718-35. DOI
82. Yu, B. C.; Jung, J. W.; Park, K.; Goodenough, J. B. A new approach for recycling waste rubber products in Li-S batteries. *Energy Environ. Sci.* **2017**, *10*, 86-90. DOI
83. Yao, L. Y.; Hou, L. P.; Song, Y. W.; et al. Recycling inactive lithium in lithium-sulfur batteries using organic polysulfide redox. *J. Mater. Chem. A*. **2023**, *11*, 7441-6. DOI